Department of Medicinal Chemistry[1], School of Pharmaceutical Science, NanChang University; People's Hospital of TongGu County[2], YiChun, JiangXi, China

Synthesis and molecular simulation study of furoic peptidomimetic derivatives as potent aminopeptodase N inhibitors

Min Gao[1], JunHua He[2], WeiDong Xu[1], XiaoPing Lai[1], Fen Liu[1], GuoGang Tu[1,*]

Received October 10, 2017, accepted November 14, 2017

**Corresponding author: GuoGang Tu, Department of Medicinal Chemistry, School of Pharmaceutical Science, NanChang University, 330006, China*
tugg110@163.com

Pharmazie 73: 123–127 (2018) *doi: 10.1691/2018.7911*

The aminopeptidase N (APN) plays a critical role in angiogenesis and is over-expressed in tumor cells. In this paper, we report the synthesis and enzyme inhibition assay of furoic peptidomimetic compounds. These new compounds exhibit potent inhibitory ability toward APN with IC_{50} values lying in the micromolar level. The binding mode of inhibitors in APN active site was explained by a molecular simulation study. These data reveal that ligand coordinating with the catalytic Zn-ion is very important for inhibitory activities.

1. Introduction

Aminopeptidase N (APN), as an ectoenzyme, is located on cell surface (Luan et al. 2007). It is a zinc-dependent metalloprotease and a type II membrane bound metalloprotease which is widely expressed in many tissues, such as epithelial cells of the kidney, fibroblasts, brain cells, intestine and liver (Breljak et al. 2003; Piela-Smith et al. 1995). The over-expression of APN is associated with many diseases, such as inflammation, viral infection and cancer. Especially it plays an important role in tumor metastasis and angiogenesis (Inagaki et al. 2010). The over-expressed APN tumor cells (such as melanoma cells and urological cancer cells) are highly motile and capable of migration through extracellular matrix (Ishii et al. 2001). Many efficient APN inhibitors have been reported, such as bestatin, probestin, and lapstatin (Repic Lampret et al. 1999).

Based on the analysis of the structural characteristic of the APN active site, it was shown that a zinc binding group (ZBG), two hydrophobic groups which can occupy the S_1 and S_1' pocket and an appropriate group which can occupy the S_2' pocket are usually necessary (Ito et al. 2006; Addlagatta et al. 2006). APN shows a broad specificity toward alanine, leucine or arginine when it preferentially releases the N-terminal neutral and basic amino acids. Furoic acid and thiadiazole derivatives have been known to exhibit broad biological properties, especially anti-tumor activities (Rzeski et al. 2007; Zeng et al. 1998). Based on the 'combination principles', the 2-furoic acid, alanine/leucine and thiadiazole were linked. A series of novel furoic peptidomimetics were synthesized and evaluated for their inhibitory activities toward APN. In addition, the binding mode of the target compounds with the APN binding site was discussed relying on docking studies, molecular dynamics (MD) simulation experiments and binding free energies calculation.

2. Investigations, results and discussion

2.1. Synthesis of the compounds

The target compounds were synthesized efficiently following the procedures shown in the Scheme. In presence of phosphorus oxychloride, the readily available carboxylic acid **1** was condensed with *N*-aminothiourea **2** to yield the 5-substituted-1,3,4-thiadiazol-2-amines **3a**-**3l** (Foroumadi et al. 1999). The amino group of amino acids **4** was protected with di-*tert*-butyl dicarbonate **5** to get Boc-amino acids **6a**-**6b** which were coupled with compounds **3a**–**3l** to led to compounds **7a**-**7u**. Then the Boc protecting group was removed to produce compounds **8a**-**8u** (Lassen et al. 2010). The 2-furoic acid **9** was reacted with $SOCl_2$ to obtain furoyl chloride **10** which without further purification was directly condensed with compounds **8a**-**8u** to get compounds **11a**-**11u** as the target compounds.

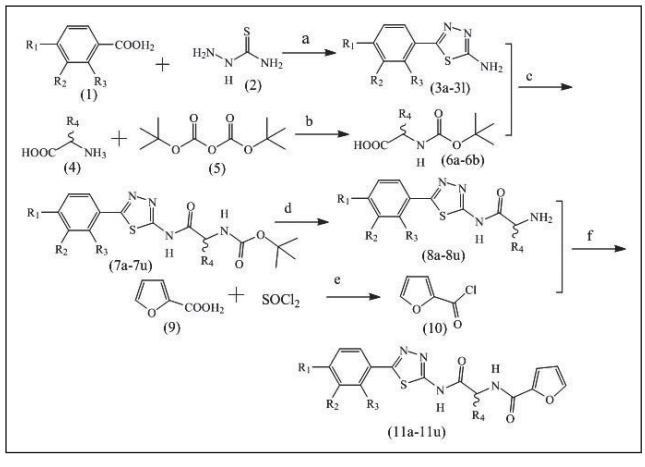

Scheme: Reagents and conditions: (a) $POCl_3$, 110°C; (b) Et_3N, r.t. (c) *N, N'*-carbonyldiimidazole, r.t.
(d) trifluoroacetic acid, r.t. (e) refluxed (f) Et_3N, r.t.

2.2. Activity testing

All the inhibition results are summarized in the Table. The results showed that most of the target compounds display moderate potency toward APN with IC_{50} values in the micromolar range. Comparing compounds **11a–11l** to **11m-11u**, we could confirm that isobutyl group introduced at the R_4-position was negatively related with the inhibitory activities. The steric effect of the substituent at the R_1-position is extremely important for potency. Compounds with a tert. butyl group (**11f**, **11r**) exhibited lower activity than compounds with a methyl group (**11d**, **11p**). For compounds **11a**-**11c**, **11l** and **11m**-**11o** introduction of a electron-withdrawing group slightly increased the activity, while electron-donating groups remarkably increased the activity. The compounds with a methoxy group (**11e**, **11q**) showed the best inhibitory activity.

Table 1: In vitro enzyme assay results for compounds 11a-11u and bestatin

Compd.	R_1	R_2	R_3	R_4	IC_{50}(μM)
11a	-H	-H	-H	$-CH_3$	93.8±8.6
11b	-Cl	-H	-H	$-CH_3$	78.4±12.7
11c	-F	-H	-H	$-CH_3$	82.7±9.3
11d	$-CH_3$	-H	-H	$-CH_3$	126.8±14.9
11e	$-OCH_3$	-H	-H	$-CH_3$	31.6±5.2
11f	$-C(CH_3)_3$	-H	-H	$-CH_3$	246.9±10.9
11g	-Br	-H	-H	$-CH_3$	172.3±7.7
11h	-H	$-CH_3$	-H	$-CH_3$	153.9±11.2
11i	-H	-Cl	-H	$-CH_3$	117.2±12.3
11j	-H	-F	-H	$-CH_3$	93.6±17.2
11k	-H	-H	-Br	$-CH_3$	268.7±10.8
11l	$-NO_2$	-H	-H	$-CH_3$	64.1±6.3
11m	-H	-H	-H	$-CH_2CH(CH_3)_2$	390.2±17.2
11n	-Cl	-H	-H	$-CH_2CH(CH_3)_2$	216.9±16.8
11o	-F	-H	-H	$-CH_2CH(CH_3)_2$	143.3±13.9
11p	$-CH_3$	-H	-H	$-CH_2CH(CH_3)_2$	178.5±7.8
11q	$-OCH_3$	-H	-H	$-CH_2CH(CH_3)_2$	47.5±5.4
11r	$-C(CH_3)_3$	-H	-H	$-CH_2CH(CH_3)_2$	276.7±18.4
11s	-Br	-H	-H	$-CH_2CH(CH_3)_2$	320.3±16.9
11t	-H	$-CH_3$	-H	$-CH_2CH(CH_3)_2$	225.4±11.1
11u	-H	-Cl	-H	$-CH_2CH(CH_3)_2$	208.9±15.8
Bestatin					6.9±0.3

To further understand the difference in bioactivity, the preferred pharmacophore docking was carried out with the highest activity and lowest activity compounds (**11e**, **11m**). As shown in Fig. 1, two compounds have been shown to recognize efficiently the S_1 and S_1' subsites of APN. The thiadiazole nitrogen of compound **11e** coordinates with the catalytic Zn-ion with the distance of 2.16 Å, and forms a hydrogen bond with polar H atom of His297. At the same time, the hydrophobic parts of aromatic rings are in contact with nonpolar surface areas of APN. In addition the catalytic Zn-ion coordinates with His297, His301 and Glu320, which is the same with the crystal structure of 2DQM. But compound **11m** only forms hydrophobic interaction and could not coordinate with the catalytic Zn-ion. So the affinity of **11e** with APN is higher than that of 11m, which leads to the better bioactivity of 11e compared to **11m**.

To further identify the critical amino acid residues for ligand binding, MD study and binding free energy calculation were performed for two docked APN-ligand complexes. The RMSD values were calculated with 5 ns trajectory to evaluate the stable binding of compounds **11e** and **11m** with APN. The RMSD values of APN backbone atoms and **11e** were about 0.1 nm and 0.04 nm, while the corresponding values of APN-11m complex were about 0.12 nm and 0.1 nm respectively. The both complexes showed a steady pattern after 2 ns. It can be seen that APN-**11e** complex is more stable than the APN-11m complex.

Among the complexes **11e** has a better free energy (-190.1 kJ/mol) binding than **11m** (-143.9 kJ/mol) as shown in Table 2. The energy difference is mainly contributed by electrostatic energy as well as polar solvation energy. The binding free energy between APN and ligands was further decomposed into the contribution of each residue using MM-PBSA approach (Fig. 2). The energy decomposition analysis shows that the main contributions of **11e** are residues Met260, Val294, Asp327, Tyr376, Tyr381 and Zn900, while the main contributions of 11m are residues Met260, Glu298, Glu320, Asp327, Tyr376, and Tyr381. It was shown that Glu298 and Glu320 are in disfavor with the binding for **11e**, and Glu121 and Arg293 are in disfavor for **11m**. Especially the contribution of the catalytic Zn-ion is in favor for **11e** but disfavor for **11m**, which leads to **11e** having more inhibitory activity than **11m**. The results of binding free energy analysis were consistent with the experimental activity.

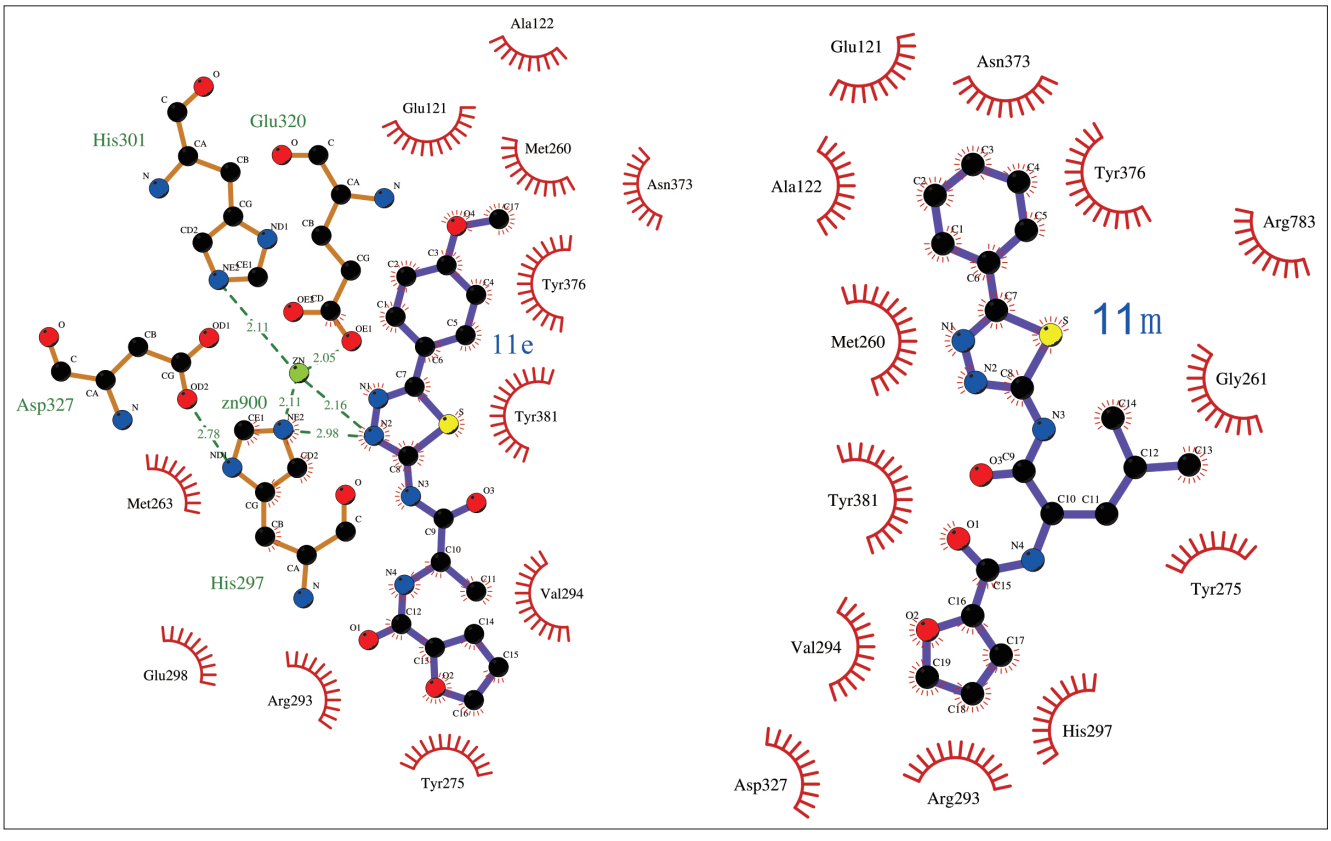

Fig. 1: Diagram (LIGPLOT) of the hydrogen bonds and hydrophobic interactions of the compounds 11e and 11m with active-site residues in *Escherichia coli* APN (PDB:2DQM)

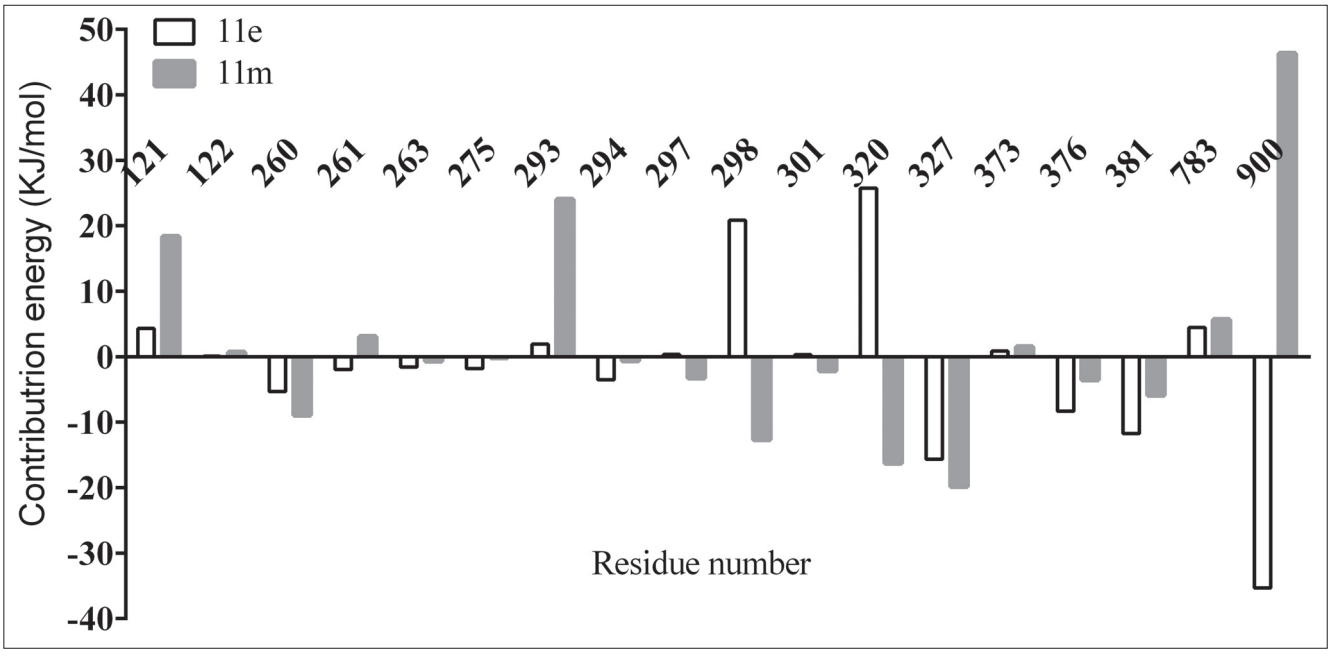

Fig. 2: Plot of binding free energy contribution per residue of both complexes

Table 2: Binding free energy and their components (kJ/mol) calculated by MM/PBSA

complex	van der waal energy	electrostatic energy	polar solvation energy	SASA energy	Binding energy
APN-11e	-177.4	-276.1	281.6	-19.0	-190.1
APN-11m	-182.6	-85.2	144.0	-20.0	-143.9

2.3. Conclusion

We developed a new series of APN inhibitors of furoic peptidomimetic derivatives. Most of the compounds have potent inhibitory activities toward APN. The compound with methoxy a group at R_4-position was found to be more potent than other target derivatives. Molecular docking, MD simulation and binding free energy calculation allow to explain possible binding modes and the difference of inhibitory activities. These data reveal that ligand coordinating with the catalytic Zn-ion is very important for inhibitory activities.

3. Experimental

3.1. Chemistry: General procedures

Unless otherwise noted, materials were used without further purification which were obtained from commercial suppliers. IR was recorded on a FTIR-8400 spectrometer. ESI-MS was determined on an Aglient-1100 series LC/MSD trap spectrometer. ^{1}HNMR spectra was obtained on a Bruker-400. Melting point was determined on a electrothermal melting point apparatus and is uncorrected.

*3.1.1. 5-Substituted-1,3,4-thiadiazol-2-amines (**3a-3l**)*

The synthetic approach to 5-substituted-1,3,4-thiadiazol-2-amine derivatives was adapted from the literature (Foronmadi et al. 1999). Briefly, a mixture of carboxylic acid derivatives (50 mmol), $POCl_3$ (13 ml) and *N*-aminothiourea (50 mmol) was reacted for 0.5 h at 75 °C. After cooling down to 0 °C, water was added. The reaction mixture was refluxed for 4 h. After reaction, the mixture was basified to pH 8 by the dropwise addition of 50% NaOH solution. The precipitate was filtered and recystallized from ethanol to get the title compounds.

*3.1.2. N-tert. Butoxycarbonyl-D-alanine (**6a**)*

To a solution of compound *D*-alanine (6.23 g, 70 mmol) and triethylamine (11.76 ml, 84 mmol) in 40 ml H_2O and 20 ml tetrahydrofuran, was added dropwise a solution of 15.28 g (70 mmol) di-*tert*-butyl dicarbonate in 20 ml tetrahydrofuran at 0 °C. The reaction mixture was stirred for 0.5 h at 0 °C, then was reacted overnight at room temperature keeping pH 8-9. After cooling to 0 °C the mixture was acidified to pH 2-3 by the dropwise addition of 2 mol/l HCl solution and extracted with ethyl acetate. The organic phase was washed with saturated brine and dried over anhydrous $MgSO_4$ and concentrated with a rotary evaporator to get the colorless oil which was stirred in petroleum ether. The white solid was filtered as the title compound. Yield: 90.9 %; mp: 80.5–81.3 °C.

*3.1.3. N-tert. Butoxycarbonyl-L-leucine (**6b**)*

To a solution of *L*-leucine (5.0 g, 38.1 mmol) in 76 ml 1 mol/l NaOH and 23 ml 1,4-dioxane was added dropwise a solution of 9.15 g (41.9 mmol) di-*tert*-butyl dicarbonate in 30 ml 1,4-dioxane at 0 °C. The reaction mixture was stirred for 0.5 h at 0 °C, then was reacted overnight at room temperature keeping pH 8-9. After reaction the mixture was diluted with 100 ml H_2O and extracted with *n*-hexane. The water phase was acidified to pH 2-3 with citric acid and extracted with ethyl acetate. The organic phase was washed with saturated brine and dried over anhydrous $MgSO_4$ and concentrated under reduced pressure to get the colorless oil as the title compound. Yield: 89.1 %.

*3.1.4. (2R)-N-(5-Phenyl-1,3,4-thiadiazol-2-yl)-2-(tertbutoxycarbonylamino)-propanamide (**7a**)*

The *N,N'*-carbonyldiimidazole was added in portions to a solution of compound **6a** (3.60 g, 19 mmol) in 60 ml tetrahydrofuran and stirred for 2 h at room temperature. The mixture was added to compound **3a** (3.81 g, 18 mmol) and stirred for 24 h at 50 °C. After reaction the solvent was removed under reduced pressure. The residual was dissolved in 30 ml ethyl acetate and washed with 1 mol/l HCl (3×50ml), H_2O (1×50ml), saturated Na_2CO_3 (3×50ml) and brine (3×50ml) in turn. The organic phase was dried over anhydrous $MgSO_4$ and concentrated under reduced pressure and recrystallized from ethanol to get the title compound as white solid. Yield: 76.1 %; mp: 127–129 °C. The other compounds (**7b**-**7u**) were synthesized by the same method.

*3.1.5. (2R)-N-(5-Phenyl-1,3,4-thiadiazol-2-yl)-2-amino-propanamide (**8a**)*

To 3.48 g (10 mmol) of compound **7a** was added dropwise a solution of 15 ml trifluoroacetic acid in 30 ml dichloromethane. The mixture was reacted for 2 h at room temperature. After reaction the solvent was removed under reduced pressure. The residual was dissolved in cooled ethyl acetate, and washed with saturated Na_2CO_3 to pH 8-9. The organic phase was dried over anhydrous $MgSO_4$ and concentrated under reduced pressure to get the title compound as white solid. Yield: 75.0 %; mp: 215–217 °C. The other compounds (**8b**-**8u**) were synthesized by the same method.

*3.1.6. 2-Furoyl chloride (**10**)*

A stirring mixture of 5.6 g (50 mmol) 2-furoic acid and 18 ml $SOCl_2$ was refluxed for 2 h, and then concentrated under reduced pressure to remove excess $SOCl_2$. The residual was dissolved in dichloromethane and concentrated under reduced pressure again to get the title compound as colorless liquid.

*3.1.7. (2R)-N-(5-Phenyl-1,3,4-thiadiazol-2-yl)-2-furoylamino-propanamide (**11a**)*

To a solution of compound **8a** (1.24 g, 5 mmol) and 4 ml triethylamine in 30 ml dichloromethane was added dropwise a solution of 5.5 mmol 2-furoyl chloride in 10 ml

dichloromethane at 0 °C. The reaction mixture was stirred for 15 min at 0 °C, then was reacted overnight at room temperature, and washed with 1 mol/l HCl (2×50ml), H_2O (1×50ml), saturated Na_2CO_3 (2×50ml) and brine (1×50ml) in turn. The organic phase was dried over anhydrous $MgSO_4$ and concentrated under reduced pressure and recrystallized from ethanol to get the target compound as white solid. Yield: 62.0 %; mp: 220–222 °C. $[\alpha]^{25}_D$ +11.98 ° (C = 0.1 M, $CHCl_3$). IR (KBr, σ/cm^{-1}): 3307, 3132, 1660, 1637, 690; ^{1}H NMR (DMSO-*d6*) δ 12.88 (s, 1H), 8.73 (d, *J* = 6.6 Hz, 1H), 7.93 (dd, *J* = 6.4, 3.0 Hz, 2H), 7.87 (d, *J* = 0.8 Hz, 1H), 7.55–7.50 (m, 3H), 7.21 (d, *J* = 3.4 Hz, 1H), 6.65 (dd, *J* = 3.4, 1.7 Hz, 1H), 4.67 (m, 1H), 1.45 (d, *J* = 7.2 Hz, 3H). ESI-MS: *m/z* [M+H]$^+$ 343. 1. The other final compounds (**11b–11u**) were obtained by the same method.

(2R)-N-[5-(4-Chlorophenyl)-1,3,4-thiadiazol-2-yl]-2-furoylamino-propanamide (*11b*): White solid, yield: 65.7%; mp: 199–201 °C. IR (KBr, σ/cm^{-1}): 3178, 1716, 1697, 1608, 1593; ^{1}H NMR (DMSO-*d6*) δ 12.92 (s, 1H), 8.73 (d, *J* = 6.6 Hz, 1H), 7.96 (d, J = 8.6 Hz, 2H), 7.88 (d, *J* = 0.9 Hz, 1H), 7.60 (d, *J* = 8.6 Hz, 2H), 7.21 (d, *J* = 3.4 Hz, 1H), 6.65 (dd, *J* = 3.4, 1.7 Hz, 1H), 4.67 (m, 1H), 1.46 (d, *J* = 7.2 Hz, 3H). ESI-MS: *m/z* [M-H]$^-$ 375.1

***(2R)-N*-[5-(4-Fluorophenyl)-1,3,4-thiadiazol-2-yl]-2-furoylamino-propanamide (*11c*):** White solid, yield: 62.6%; mp: 176–177 °C. IR (KBr, σ/cm^{-1}): 3153, 1705, 1647, 1595, 661; ^{1}H NMR (DMSO-*d6*) δ 12.89 (s, 1H), 8.73 (d, *J* = 6.6 Hz, 1H), 8.07–7.93 (m, 2H), 7.87 (d, *J* = 0.9 Hz, 1H), 7.37 (dd, *J* = 12.3, 5.4 Hz, 2H), 7.21 (d, *J* = 3.4 Hz, 1H), 6.65 (dd, *J* = 3.4, 1.7 Hz, 1H), 4.66 (m, 1H), 1.45 (d, *J* = 7.2 Hz, 3H). ESI-MS: *m/z* [M+H]$^+$361.1

***(2R)-N*-[5-(4-Methylphenyl)-1,3,4-thiadiazol-2-yl]-2-furoylamino-propanamide (*11d*):** White solid, yield: 61.4%; mp: 221–223 °C. IR (KBr, σ/cm^{-1}): 3408, 3132, 1683, 1654, 1635, 669; ^{1}H NMR (DMSO-*d6*) δ 12.83 (s, 1H), 8.71 (d, *J* = 6.5 Hz, 1H), 7.84 (dd, *J* = 21.1, 9.0 Hz, 3H), 7.34 (d, *J* = 7.9 Hz, 2H), 7.21 (d, *J* = 3.2 Hz, 1H), 6.65 (d, *J* = 1.5 Hz, 1H), 4.67 (m, 1H), 2.36 (s, 3H), 1.45 (d, *J* = 7.2 Hz, 3H). ESI-MS: *m/z* [M+H]$^+$ 357.1

***(2R)-N*-[5-(4-Methoxyphenyl)-1,3,4-thiadiazol-2-yl]-2-furoylamino-propanamide (*11e*):** White solid, yield: 62.7%; mp: 161–162 °C. IR (KBr, σ/cm^{-1}): 3408, 1697, 1683, 1654, 669; ^{1}H NMR (DMSO-*d6*) δ 12.78 (s, 1H), 8.70 (d, *J* = 6.6 Hz, 1H), 7.90–7.85 (m, 3H), 7.21 (dd, *J* = 3.5, 0.8 Hz, 1H), 7.10–7.06 (m, 2H), 6.65 (dd, *J* = 3.5, 1.8 Hz, 1H), 4.70–4.64 (m, 1H), 3.82 (s, 3H), 1.45 (d, *J* = 7.2 Hz, 3H). ESI-MS: *m/z* [M+H]$^+$ 373.1

***(2R)-N*-[5-(4-Tertbutylphenyl)-1,3,4-thiadiazol-2-yl]-2-furoylamino-propanamide (*11f*):** White solid, yield: 63.1%; mp: 223–225 °C. $[\alpha]^{25}_D$ +21.87 ° (C = 0.1 M, $CHCl_3$). IR (KBr, σ/cm^{-1}): 3282, 3143, 1714, 1647, 682; ^{1}H NMR (DMSO-*d6*) δ 12.86 (s, 1H), 8.72 (d, *J* = 6.6 Hz, 1H), 7.87 (dd, *J* = 11.3, 4.6 Hz, 3H), 7.55 (d, *J* = 8.5 Hz, 2H), 7.22 (d, *J* = 3.4 Hz, 1H), 6.65 (dd, *J* = 3.4, 1.7 Hz, 1H), 4.67 (m, 1H), 1.45 (d, *J* = 7.2 Hz, 3H), 1.31 (s, 9H). ESI-MS: *m/z* [M+H]$^+$ 399.1

***(2R)-N*-[5-(4-Bromophenyl)-1,3,4-thiadiazol-2-yl]-2-furoylamino-propanamide (11g):** White solid, yield: 67.3%; mp: 218–220 °C. IR (KBr, σ/cm^{-1}): 3417, 3091, 1716, 1697, 1635; ^{1}H NMR ($CDCl_3$) δ 8.03 (d, *J* = 6.6 Hz, 1H), 7.87 (d, *J* = 8.5 Hz, 2H), 7.68 (d, *J* = 8.5 Hz, 2H), 7.20 (s, 1H), 7.12 (d, *J* = 3.5 Hz, 1H), 6.43 (d, *J* = 1.7 Hz, 1H), 4.99 (m, 1H), 1.72 (d, *J* = 7.3 Hz, 3H). ESI-MS: *m/z* [M-H]$^-$ 421.0

***(2R)-N*-[5-(3-Methylphenyl)-1,3,4-thiadiazol-2-yl]-2-furoylamino-propanamide (*11h*):** White solid, yield: 64.8%; mp: 193–195 °C. IR (KBr, σ/cm^{-1}): 3313, 3151, 1714, 1631, 686; ^{1}H NMR (DMSO-*d6*) δ 12.86 (s, 1H), 8.73 (d, *J* = 6.6 Hz, 1H), 7.87 (d, *J* = 0.9 Hz, 1H), 7.80–7.68 (m, 2H), 7.41 (t, *J* = 7.6 Hz, 1H), 7.33 (d, *J* = 7.6 Hz, 1H), 7.21 (d, *J* = 3.4 Hz, 1H), 6.65 (dd, *J* = 3.4, 1.7 Hz, 1H), 4.66 (m, 1H), 2.38 (s, 3H), 1.45 (d, *J* = 7.2 Hz, 3H). ESI-MS: *m/z* [M+H]$^+$357.1

***(2R)-N*-[5-(3-Chlorophenyl)-1,3,4-thiadiazol-2-yl]-2-furoylamino-propanamide (*11i*):** White solid, yield: 64.8%; mp: 196–197 °C. IR (KBr, σ/cm^{-1}): 3300, 3145, 1699, 1660, 1659, 686; ^{1}H NMR (DMSO-*d6*) δ 12.94 (s, 1H), 8.72 (d, *J* = 6.6 Hz, 1H), 7.99 (t, *J* = 1.8 Hz, 1H), 7.92– 7.85 (m, 2H), 7.65–7.50 (m, 2H), 7.21 (dd, *J* = 3.5, 0.7 Hz, 1H), 6.65 (dd, *J* = 3.5, 1.8 Hz, 1H), 4.68 (m, 1H), 1.46 (d, *J* = 7.2 Hz, 3H). ESI-MS: *m/z* [M+H]$^+$377.0

***(2R)-N*-[5-(3-Fluorophenyl)-1,3,4-thiadiazol-2-yl]-2-furoylamino-propanamide (*11j*):** White solid, yield: 64.8%; mp: 196–197 °C. IR (KBr, σ/cm^{-1}): 3425, 1697, 1636, 1593, 682; ^{1}H NMR (DMSO-*d6*) δ 12.95 (s, 1H), 8.74 (d, *J* = 6.5 Hz, 1H), 7.87 (s, 1H), 7.82–7.72 (m, 2H), 7.58 (dd, *J* = 8.2, 6.1 Hz, 1H), 7.37 (dd, *J* = 8.4, 1.8 Hz, 1H), 7.21 (d, *J* = 3.4 Hz, 1H), 6.65 (dd, *J* = 3.4, 1.7 Hz, 1H), 4.67 (m, 1H), 1.45 (d, *J* = 7.2 Hz, 3H). ESI-MS: *m/z* [M+H]$^+$ 361.1

***(2R)-N*-[5-(2-Bromophenyl)-1,3,4-thiadiazol-2-yl]-2-furoylamino-propanamide (*11k*):** White solid, yield: 66.2%; mp: 204–206 °C. IR (KBr, σ/cm^{-1}): 3365, 3134, 1699, 1697, 1652, 705; ^{1}H NMR (DMSO-*d6*) δ 12.94 (s, 1H), 8.72 (d, *J* = 6.5 Hz, 1H), 7.93 (dd, *J* = 7.8, 1.6 Hz, 1H), 7.88 (d, *J* = 0.9 Hz, 1H), 7.86–7.82 (m, 1H), 7.59–7.52 (m, 1H), 7.48 (dd, *J* = 7.8, 1.7 Hz, 1H), 7.21 (d, *J* = 3.4 Hz, 1H), 6.65 (dd, *J* = 3.4, 1.7 Hz, 1H), 4.71–4.64 (m, 1H), 1.46 (d, *J* = 7.2 Hz, 3H). ESI-MS: m/z [M+H]$^+$ 423.0

***(2R)-N*-[5-(4-Nitrophenyl)-1,3,4-thiadiazol-2-yl]-2-furoylamino- propanamide (*11l*):** Yellow solid, yield: 57.3%; mp: 250–251 °C. IR (KBr, σ/cm^{-1}): 3390, 1716, 1697, 1635, 1524, 1338, 686; ^{1}H NMR (DMSO-*d6*) δ 13.06 (s, 1H), 8.75 (d, *J* = 6.6 Hz, 1H), 8.43–8.29 (m, 2H), 8.27 – 8.15 (m, 2H), 7.89 (dd, *J* = 1.7, 0.8 Hz, 1H), 7.21 (dd, *J* = 3.5, 0.8 Hz, 1H), 6.66 (dd, *J* = 3.5, 1.7 Hz, 1H), 4.69 (d, *J* = 7.2 Hz, 1H), 1.47 (d, *J* = 7.2 Hz, 3H). ESI-MS: *m/z* [M-H]$^-$ 386.1

***(2S)-N*-(5-Phenyl-1,3,4-thiadiazol-2-yl)-2-furoylamino-4-methyl-pentanamide (*11m*):** White solid, yield: 66.2%; mp: 204–206 °C. IR (KBr, σ/cm^{-1}): 3175, 3033, 1733, 1635, 688cm; ^{1}H NMR (DMSO-*d6*) δ 12.95 (s, 1H), 8.65 (d, *J* = 7.5 Hz, 1H), 7.94–7.92 (m, 2H), 7.88 (dd, *J* = 1.7, 0.8 Hz, 1H), 7.53 (dd, *J* = 5.1, 1.8 Hz, 3H), 7.23 (dd, *J* = 3.5, 0.7 Hz, 1H), 6.65 (dd, *J* = 3.5, 1.7 Hz, 1H), 4.77–4.72 (m, 1H), 1.83 (ddd, J = 13.3, 10.9, 4.7 Hz, 1H), 1.76–1.68 (m, 1H), 1.59 (ddd, J = 13.5, 9.1, 4.5 Hz, 1H), 0.92 (dd, *J* = 18.0, 6.6 Hz, 6H). ESI-MS: *m/z* [M+H]$^+$ 385.1

***(2S)-N*-[5-(4-Chlorophenyl)-1,3,4-thiadiazol-2-yl]-2-furoylamino-4-methyl-pentanamide (*11n*):** White solid, yield: 70.9%; mp: 201–202 °C. IR (KBr, σ/cm^{-1}): 3282, 3143, 1697, 1664, 1591, 680; ^{1}H NMR ($CDCl_3$) δ 8.65–8.50 (m, 1H), 8.06 (s, 1H), 7.86 (d, *J* = 7.3 Hz, 1H), 7.49 (d, *J* = 15.4, 7.9 Hz, 2H), 7.05 (d, *J* = 2.2 Hz, 2H), 6.37 (s, 1H), 4.99–4.88 (m, 1H), 2.00 (t, J = 9.2 Hz, 2H), 1.83 (dd, *J* = 10.3, 5.5 Hz, 1H), 1.10–0.98 (m, 6H). ESI-MS: *m/z* [M+H]$^+$ 419.1

***(2S)-N*-[5-(4-Fluorophenyl)-1,3,4-thiadiazol-2-yl]-2-furoylamino-4-methyl-pentanamide (*11o*):** White solid, yield: 61.7%; mp: 193–194 °C. IR (KBr, σ/cm^{-1}): 3130, 2958, 1733, 1637, 1593, 659; ^{1}H NMR ($CDCl_3$) δ 8.65 (d, *J* = 6.7 Hz, 1H), 8.02 (dd, *J* = 7.7, 5.3 Hz, 2H), 7.29–7.20 (m, 2H), 7.08–6.98 (m, 2H), 6.36 (d, *J* = 1.5 Hz, 1H), 4.94 (dd, *J* = 10.2, 6.3 Hz, 1H), 2.06–1.90 (m, 2H), 1.83 (dd, *J* = 11.4, 6.2 Hz, 1H), 1.00 (dd, *J* = 10.0, 6.2 Hz, 6H). ESI-MS: *m/z* [M+H]$^+$403.1

***(2S)-N*-[5-(4-Methylphenyl)-1,3,4-thiadiazol-2-yl]-2-furoylamino-4-methyl-pentanamide (*11p*):** White solid, yield: 64.9%; mp: 184–186 °C, $[\alpha]^{25}_D$ -162.33 (C=0.1 M, $CHCl_3$). IR (KBr, σ/cm^{-1}): 3153, 2956, 1697, 1635, 1593; ^{1}H NMR ($CDCl_3$) δ 8.89 (d, *J* = 6.9 Hz, 1H), 7.91 (d, *J* = 7.7 Hz, 2H), 7.34 (d, *J* = 7.8 Hz, 2H), 7.02 (d, *J* = 2.6 Hz, 1H), 6.96 (s, 1H), 6.32 (d, *J* = 1.5 Hz, 1H), 4.98–4.85 (m, 1H), 2.45 (s, 3H), 2.10–1.91 (m, 2H), 1.82 (dd, *J* = 11.6, 6.6 Hz, 1H), 1.00 (t, *J* = 6.3 Hz, 6H). ESI-MS: *m/z* [M+H]$^+$ 399.1

***(2S)-N*-[5-(4-Methoxyphenyl)-1,3,4-thiadiazol-2-yl]-2-furoylamino-4-methyl-pentanamide (*11q*):** White solid, yield: 59.2%; mp: 188–190 °C, $[\alpha]^{25}_D$ -161.02 (C=0.1 M, $CHCl_3$). IR (KBr, σ/cm^{-1}): 3311, 3153, 1701, 1662, 1596; ^{1}H NMR ($CDCl_3$) δ 8.89 (s, 1H), 7.96 (d, *J* = 8.7 Hz, 2H), 7.05 (s, 1H), 7.02 (d, *J* = 4.6 Hz, 2H), 6.98 (s, 1H), 6.32 (dd, *J* = 3.4, 1.7 Hz, 1H), 4.90 (dd, *J* = 10.1, 6.0 Hz, 1H), 3.90 (s, 3H), 2.07–1.93 (m, 2H), 1.85–1.76 (m, 1H), 1.00 (t, *J* = 6.9 Hz, 6H). ESI-MS: *m/z* [M+H]$^+$ 415.1

***(2S)-N*-[5-(4-Tertbutylphenyl)-1,3,4-thiadiazol-2-yl]-2-furoylamino-4-methyl-pentanamide (*11r*):** White solid, yield: 59.7%; mp: 240–242 °C, $[\alpha]^{25}_D$ -127.90 (C=0.1 M, $CHCl_3$). IR (KBr, σ/cm^{-1}): 3298, 3147, 1662, 1593, 680; ^{1}H NMR ($CDCl_3$) δ 8.81 (s, 1H), 7.95 (d, *J* = 8.4 Hz, 2H), 7.55 (d, *J* = 8.4 Hz, 2H), 7.08–6.96 (m, 2H), 6.33 (dd, *J* = 3.4, 1.7 Hz, 1H), 4.90 (dd, *J* = 10.3, 6.9 Hz, 1H), 2.01 (d, *J* = 7.3 Hz, 2H), 1.82 (s, 1H), 1.38 (s, 10H), 1.01 (t, *J* = 6.0 Hz, 6H). ESI-MS: *m/z* [M+H]$^+$441.2

***(2S)-N*-[5-(4-Bromophenyl)-1,3,4-thiadiazol-2-yl]-2-furoylamino-4-methyl-pentanamide (*11s*):** White solid, yield: 62.8%; mp: 138–140 °C. IR (KBr, σ/cm^{-1}): 3134, 2956, 1716, 1697, 1637; ^{1}H NMR ($CDCl_3$) δ 8.31 (s, 1H), 7.87 (d, *J* = 8.5 Hz, 2H), 7.68 (d, *J* = 8.5 Hz, 2H), 7.12–7.06 (m, 2H), 6.39 (dd, *J* = 3.4, 1.6 Hz, 1H), 4.92 (s, 1H), 1.95 (d, *J* = 7.5 Hz, 2H), 1.85 (d, *J* = 12.3 Hz, 1H), 1.01 (t, *J* = 5.6 Hz, 6H). ESI-MS: *m/z* [M+H]$^+$465.1

***(2S)-N*-[5-(3-Methylphenyl)-1,3,4-thiadiazol-2-yl]-2-furoylamino-4-methyl-pentanamide (*11t*):** White solid, yield: 61.5%; mp: 209–210 °C. IR (KBr, σ/cm^{-1}): 3274, 3126, 1749, 1664, 1589, 690; ^{1}H NMR ($CDCl_3$) δ 8.86 (d, *J* = 6.8 Hz, 1H),7.83 (d, *J* = 6.1 Hz, 2H), 7.42 (t, *J* = 7.9 Hz, 1H), 7.35 (d, *J* = 7.5 Hz, 1H), 7.02 (d, *J* = 2.9 Hz, 1H), 6.98 (s, 1H), 6.33 (dd, *J* = 3.3, 1.6 Hz, 1H), 4.91 (dd, *J* = 10.6, 6.8 Hz, 1H), 2.45 (s, 3H), 2.11–1.94 (m, 2H), 1.82 (dd, *J* = 10.4, 5.5 Hz, 1H), 1.02 (t, *J* = 5.8 Hz, 6H). ESI-MS: *m/z* [M+H]$^+$ 399.1

***(2S)-N*-[5-(3-Chlorophenyl)-1,3,4-thiadiazol-2-yl]-2-furoylamino-4-methyl-pentanamide (*11u*):** White solid, yield: 58.4%; mp: 196–198 °C. IR (KBr, σ/cm^{-1}): 3178, 3031, 2956, 1716, 1697, 1637, 1595, 682; ^{1}H NMR (DMSO-*d6*) δ 13.03 (s, 1H), 8.67 (d, *J* = 7.5 Hz, 1H), 7.99 (t, *J* = 1.7 Hz, 1H), 7.90–7.86 (m, 2H), 7.61–7.54 (m, 2H), 7.23–7.21 (m, 1H), 6.65 (dd, *J* = 3.4, 1.7 Hz, 1H), 4.79 – 4.71 (m, 1H), 1.83 (ddd, *J* = 13.4, 10.9, 4.7 Hz, 1H), 1.75–1.68 (m, 1H), 1.59 (ddd, *J* = 13.5, 9.2, 4.5 Hz, 1H), 0.92 (dd, *J* = 18.2, 6.6 Hz, 6H). ESI-MS: *m/z* [M+H]$^+$419.0

3.2. In-vitro APN inhibition assay

Inhibitory activity toward APN was determined by hydrolysis substrate in 50 mM PBS (pH 7.2) (Jin et al. 2013). The enzyme is microsomal aminopeptidase from Porcine Kidney Microsomes and the substrate is *L*-leu-*p*-nitroanilide. After adding the target compounds with various concentrations, the solution was incubated with APN for 5 min at 37 °C. Then the solution of substrate was added into the above mixture, which was incubated for another 30 min at 37 °C. Under 405 nm wavelength the resulting solution was detected to gain absorption.

3.3. Molecular docking

It is necessary to elucidate of ligand binding mechanisms. Molecular docking and molecular dynamics were studied. The critical amino acid residues were identified for the most active compound **11e** and the least active compound **11m** with APN (PDBid: 2DQM). Docking of two compounds to APN was carried out by AutoDock4.2 software package with a standard protocol (Morris et al. 1998). All torsion angles for compounds were considered flexible. In order to include not only the active site but also significant portions of the surrounding surface, the dimensions of the grids were set to be sufficiently large for 60×60×60 Å with AutoGrid.

3.4. Molecular dynamics simulation

Based on the docking results, MD simulation was carried out with the gromacs 4.6.5 (Van Der Spoel et al. 2005). The APN-**11e** and APN-**11m** complex were placed in the center of an octahedron box, neutralized by adding suitable counterions and solvated by TIP3P water with amber99SB force field (Hornak et al. 2006). The v-rescale temperature coupling and parrinello-rahman pressure coupling were used in the NPT ensemble. The nominal charge of +2 was used for the catalytic Zn-ion which was maintained in the correct ligation state by distance restraints. The Zn-chelating histidine residues were protonated at the δ-nitrogen (Manzetti et al. 2003). The complexes were first energy minimized with the steepest descent method; then a 100 ps position restraining simulation was carried out to relieve close contacts; finally a 5 ns MD simulation was performed. Periodic boundary conditions were applied to avoid edge effects.

3.5. Binding free energy calculation

For two complex systems, free energy calculations were performed by g_mmpbsa for 200 snapshots which were extracted from the last 2 ns stable MD trajectory (Kumari et al. 2014). The van der Waals radius of the catalytic Zn-ion was set to 1.6 (Sakharov et

al. 2005). The free energy of each snapshot was calculated for each molecular species (complex, ligand and protein), then the binding free energy (ΔG_{bind}) was calculated by Eq. (1). The molecular mechanics energy (ΔG_{MM}) was calculated by the van der Waals and electrostatic interactions. The solvation free energy (ΔG_{sol}) was composed of the nonpolar and the polar contributions. Nonpolar salvation free energy was obtained by Solvent Accessible Surface Area (SASA) model, whereas polar solvation free energy could be determined with MM/PBSA method by solving the poisson-boltzmann equation. $T\Delta S$ represented the entropy term:

$\Delta G_{bind} = \Delta G_{MM} + \Delta G_{sol} - T\Delta S$ (1)

Acknowledgments: The project was supported by the Jiangxi Province Science Foundation (20171BAB205104) and National Natural Science Foundation of China (81160383, 81260469).

Conflict of interest: The author(s) confirm that this article content has no conflict of interest.

References

Addlagatta A, Gay L, Matthews BW (2006) Structure of aminopeptidase N from Escherichia coli suggests a compartmentalized, gated active site. Proc Natl Acad Sci USA 103: 13339-13344.

Breljak D, Gabrilovac J, Boranic´ M (2003) Aminopeptidase N/CD13 and haematopoietic cells. Haema 6: 453-461.

Foroumadi A, Daneshtalab M, Shafiee A (1999) Synthesis and in vitro antifungal activity of 2-aryl-5-phenylsulfonyl-1,3,4-thiadiazole derivatives. Arzneimittel-Forschung 49: 1035-1038.

Hornak V, Abel R, Okur A, Strockbine B, Roitberg A, Simmerling C (2006) Comparison of multiple amber force fields and development of improved protein backbone parameters. Proteins 65: 712-725.

Inagaki Y, Tang W, Zhang L, Du G, Xu W, Kokudo N (2010) Novel aminopeptidase N (APN/CD13) inhibitor 24F can suppress invasion of hepatocellular carcinoma cells as well as angiogenesis. Biosci Trends 4: 56-60.

Ishii K, Usui S, Sugimura Y, Yoshida S, Hioki T, Tatematsu M, Yamamoto H, Hirano K (2001) Aminopeptidase N regulated by zinc in human prostate participates in tumor cell invasion. Int J Cancer 92: 49-54.

Ito K, Nakajima Y, Onohara Y, Takeo M, Nakashima K, Matsubara F, Ito T, Yoshimoto T (2006) Crystal structure of aminopeptidase N (proteobacteria alanyl aminopeptidase) from Escherichia coli and conformational change of methionine 260 involved in substrate recognition. J Biol Chem 281: 33664-33676.

Jin K, Zhang XP, Ma CH, Xu YY, Yuan YM, Xu WF (2013) Novel indoline-2,3-dione derivatives as inhibitors of aminopeptidase N (APN). Bioorg Med Chem 21: 2663-2670.

Kumari R, Kumar R, Open Source Drug Discovery Consortium and Lynn A (2014) *g_mmpbsa*—A GROMACS tool for high-throughput MM-PBSA calculations. J Chem Inf Model 54: 1951-1962.

Lassen KM, Lee J, Joullié MM (2010) Synthetic studies of tamandarin B side chain analogues. J Org Chem 75: 3027-3036.

Luan Y, Xu W (2007) The structure and main functions of aminopeptidase N. Curr Med Chem 14: 639-647.

Manzetti S, McCulloch DR, Herington AC, van der Spoel D (2003) Modeling of enzyme–substrate complexes for the metalloproteases MMP-3, ADAM-9 and ADAM-10. J Comput Aided Mol Des 17: 551-565.

Morris GM, Goodsell DS, Halliday RS, Huey R, Hart WE, Belew RK, Olson AJ (1998) Automated docking using a Lamarckian genetic algorithm and an empirical binding free energy function. J Comput Chem 19: 1639-1662.

Piela-Smith TH, Korn JH (1995) Aminopeptidase N: a constitutive cell-surface protein on human dermal fibroblasts. Cell Immunol 162: 42-48.

Repic Lampret B, Kidric J, Kralj B, Vitale L, Pokorny M, Renko M (1999) Lapstatin, a new aminopeptidase inhibitor produced by Streptomyces rimosus, inhibits autogenous aminopeptidases. Arch Microbiol 171: 397-404.

Rzeski W, Matysiak J, Kandefer-Szerszen M (2007) Anticancer, neuroprotective activities and computational studies of 2-amino-1,3,4-thiadiazole based compound. Bioorg Med Chem 15: 3201-3207.

Sakharov DV, Lim C (2005) Zn protein simulations including charge transfer and local polarization effects. J Am Chem Soc 127: 4921-4929.

Van Der Spoel D, Lindahl E, Hess B, Groenhof G, Mark AE, Berendsen HJ (2005) GROMACS: Fast, flexible, and free. J Comput Chem 26: 1701-1718.

Zeng LR, Zhu Y, Yan SJ, Su JY (1998) A new furanolactam from the Chinese sponge Phacellis fusca. Chem Res Chin Univ 14: 426-427.